Effect of annealing on photovoltaic performance of fabricated planar organic-inorganic perovskite solar cells

Ali Baltakesmez[1,2], Mehmet Biber[1] and Sebahattin Tüzemen[1]

[1]Department of Physics, Faculty of Science, Atatürk University, 25240 Erzurum, Turkey
[2]Department of Physics, Faculty of Science, Çankırı Karatekin University, 18100 Çankırı, Turkey

E-mail: baltakesmez@atauni.edu.tr

Abstract. We fabricated planar perovskite solar cells used $CH_3NH_3PbI_{3-x}Cl_x$ for light harvesting to investigate effect of annealing on photovoltaic performance of fabricated device. The devices have an architecture of Glass/ITO/Pedot:PSS/Perovskite/$PC_{61}BM$/Al. Layers of hole transport (Pedot:PSS), active and electron transport ($PC_{61}BM$) were prepared from solution based one step deposition method by a spin coater and standard annealing procedure. The current−voltage curves of devices were measured inside the glovebox using a Keithley 2400 sourcemeter. The cells were illuminated by a solar simulator have optical intensity value of 300 mW/cm^2. For the best cells, while PCE value of 5.78% before the annealing, photovoltaic efficiency was improved average 13% delivered a short-circuit current density of 3.20 mA/cm^2, open-circuit voltage of 0.82 V and fill factor of 0.74, leading to an efficiency of 6.54% with respect to prior to annealing.

1. Introduction

Organic-inorganic lead three or mixed-halide perovskite ($CH_3NH_3PbI_3$ or $CH_3NH_3PbI_{3-x}Cl_x$) based solar cells (PSCs) have been considered as a promising devices for next-generation due to their high power conversion efficiency (PCE) along with low cost and low temperature fabrication. As a light harvester, $CH_3NH_3PbI_3$ and $CH_3NH_3PbI_{3-x}Cl_x$ have several advantages such as a direct band gap, a large absorption coefficient, a low exciton bonding energy, high carrier mobility and long electron–hole diffusion lengths of 100 nm and 1 μm, respectively [1-2].

The first reported organometal perovskite based device with the PCE of 3.8% is a liquid electrolyte based cell [3]. Since the first report on a long-term durable perovskite active layer based solar cells were reported with ever-growing efficiency and the PCE climbed the certified non-stabilized efficiency of 20.1%, in 2014 [4]. According to the reported studies to obtain the high efficiency device, the all layers and the metal contact should be not only free from pinhole but also good contact between the adjacent layers to lower the series resistance and higher the shunt resistance [4-8].

In this study, we present the perovskite solar cells were fabricated by the one-step spin-coating process comprising changed performance parameters of the fabricated cell with the annealing. Optical and structural characterizations show that the coated perovskite thin films have suitable properties as a light absorber. We observed significant changing efficiency with the annealing after the fabrication.

2. Experimental

Indium tin oxide (ITO) coated glass substrates with a sheet resistance of ~15 Ωsq^{-1} were cut in the dimensions of 1.25x1.25 cm. Then they were patterned by etching with 10wt% HCl solution for about 2 h. The patterned ITO substrates were cleaned by the following procedure: sonication in detergent (15 min), sonication in acetone (15min) and sonication in propanol (15 min), respectively and rinsed with distilled water before each the solvent. Afterward, for using as a hole transport layer (HTL), 5% DMSO added Poly(3,4-ethylenedioxythiophene) poly(styrene -sulfonate) (PEDOT:PSS (PH500)) was

spin coated onto the substrates and then the films were thermally annealing at 120 ^{o}C for 25 min in atmosphere.

The solutions and deposition of the other layers including the perovskite, the electron transport (ETL) and the cathode electrode were carried out in the Ar glovebox (O_2: <1 ppm and H_2O: <1 ppm). Methylammonim iodide (CH_3NH_3I (Dyesol)) and lead (II) chloride ($PbCl_2$ (Aldrich)) were dissolved in a anhydrous N,N-dimethylformamide (DMF) to be used as the perovskite precursor which is 40wt% solution prepared from $PbCl_2$ (0.8 M) and CH_3NH_3I (2.6 M) in a molar ratio of 1:3 and the solution stirred at 60^{o}C for a day.

The perovskite layer was deposited by spin-casting 100 µl of the precursor solution onto the substrate of PEDOT:PSS/ITO/glass at 3000 rpm for 30 s. The films were thermally annealing at 90 ^{o}C for 90 min and then color of the films converted from yellowish to dark brownish. After the films cooled to the room temperature, PCBM layer was deposited on top of the perovskite films from 20 mg/ml chlorobenzene solution at 2000 rpm for 45 s. Finally, a 100 nm thick Al film was evaporated on top of the PCBM layer with rate of 1 A/s to form the back contact of the devices. The fabricated cells were annealed 65^{o}C after the electrical measurements to observe effect of the annealing. The active area of the devices was 0.3 cm^2.

The devices were characterized under AM 1.5G solar simulator with light intensity of 300 mV/cm^2. The current density-voltage (J-V) curves were using a Keithley 2400 source-measurement system. The optical properties of the perovskite film were studied by Perkin-Elmer UV-visible spectrometry (LAMBDA 2S). The X-ray diffraction studies for structural perovskite film has been done by the diffractometer have a wavelength of 1.54059 A.

3. Results and discussion

Fig. 1(a) shows the optical absorbance of the perovskite film deposited on the PEDOT:PSS/ITO/glass substrate by spin-coating. It can be seen from this figure that the active layer absorbs a wide range of light from visible to the near infrared with an absorption onset at 780 nm. Additionally, the absorbance spectra is converted to absorption coefficients as a function of the photon energy hν and is plotted as shown in the Fig. 1(b). The optical band gap (E_g) estimated from Fig. 1(b) and is found to be 1.55 eV that is agreement with published results for $CH_3NH_3PbI_3$ or $CH_3NH_3PbI_{3-x}Cl_x$ in literature [9].

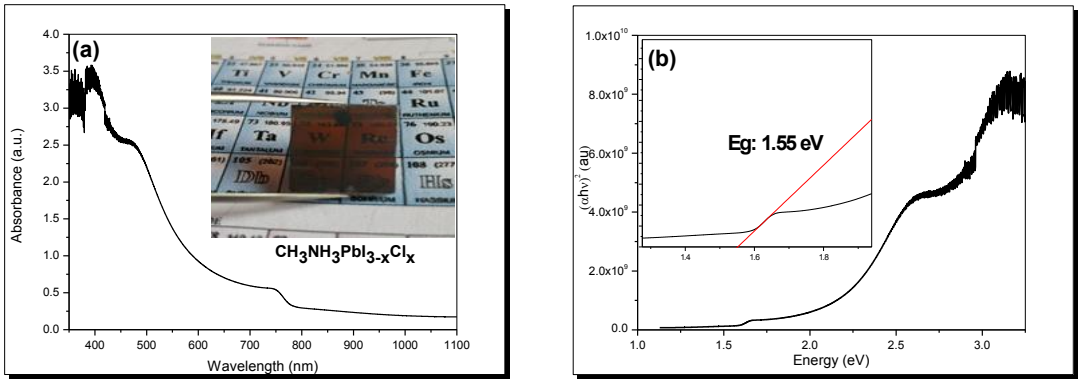

Fig.1. (a) Image of perovskite film on the PEDOT:PSS/ITO/glass and UV−visible absorbance spectra of the thin films. (b) The spectra of absorption coefficients as a function of the photon energy hν.

The structure of the resulting $CH_3NH_3PbI_{3-x}Cl_x$ mixed halide perovskite films was investigated by X-ray diffraction (XRD) as shown in Fig. 2. The XRD pattern of the spin coated film revealed the presence of two dominant peaks at the following 2θ values: 13.44° and 27.72°. These peaks correspond to the reflections from the (110) and (220) lattice planes that indicates the formation of the orthorhombic crystal structure [10].

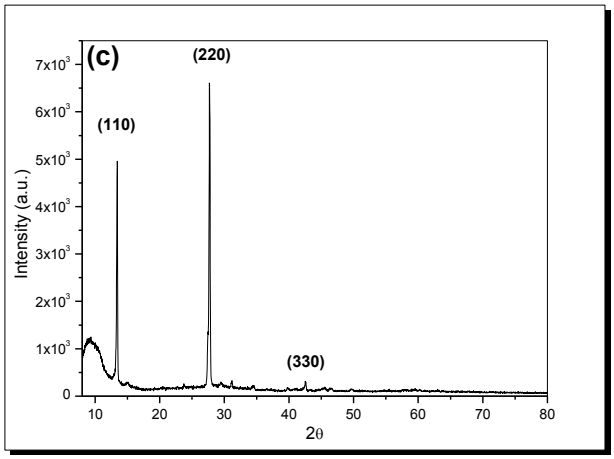

Fig.2. XRD pattern of a mixed halide perovskite $CH_3NH_3PbI_{3-x}Cl_x$ film.

Fig. 3 (a) shows a schematic diagram of the fabricated ITO/PEDOT:PSS/perovskite/PCBM/Al planar structured cells. As show in Fig 3 (b), the devices have the characteristic of a rectifying behavior in the dark. Moreover, under an illumination of 300 mW/cm^2, the current-voltage (J-V) characteristic of the devices is given in Fig 3 (c) and (d), that shows the change of the J-V characteristic before and after the annealing. The performance parameters of the devices are also summarized in Table 1.
The device I has a short-circuit current density (J_{sc}) of 2.36 mA/cm^2, an open-circuit voltage (V_{oc}) of 0.90 V and a fill factor (FF) of 71.5%, yielding an efficiency (η) of 5.07%. However, the annealed device I has a J_{sc} of 3.04 mA/cm^2, a V_{oc} of 0.84 V and a FF of 74.0%, leading to an efficiency of 6.31%. The effect of the annealing on the devices was significantly observed as improvement of current transport and the both resistance of the device as seen in the Table 1. The enhanced current transport is generally connected with decreased recombination of the photo-generated free carriers at the interfaces of the transport layers, passivated short-circuit current or the lower series resistance between the layer and the metal contact. In the our measurements for the device I, the value of FF increased from 71.5% to 74.0% dependent on the both resistances of the device while the V_{oc} decreased 60 mV. Furthermore, the all performance parameters of the device II are better than before annealing, particularly at the FF and the efficiency. Therefore, the improvement of the performance can mainly attribute to the improved resistance of both series and shunt. Additionally, the carrier mobility might be enhanced between grains and also the interface states, which can be generated by a large density of crystal defects close to interface of the layers.

Table 1. The performance parameters of the cells after and before annealing.

Device	Annealing	J_{sc} (mA/cm^2)	V_{oc} (V)	FF (%)	η (%)	R_{sh}(kΩcm^2)	R_s(Ωcm^2)
I	Before	2.36	0.90	71.5	5.07	19.20	60
	After	3.04	0.84	74.0	6.31	39.24	43
II	Before	3.02	0.80	71.6	5.78	248.67	37
	After	3.20	0.82	74.9	6.54	313.22	32

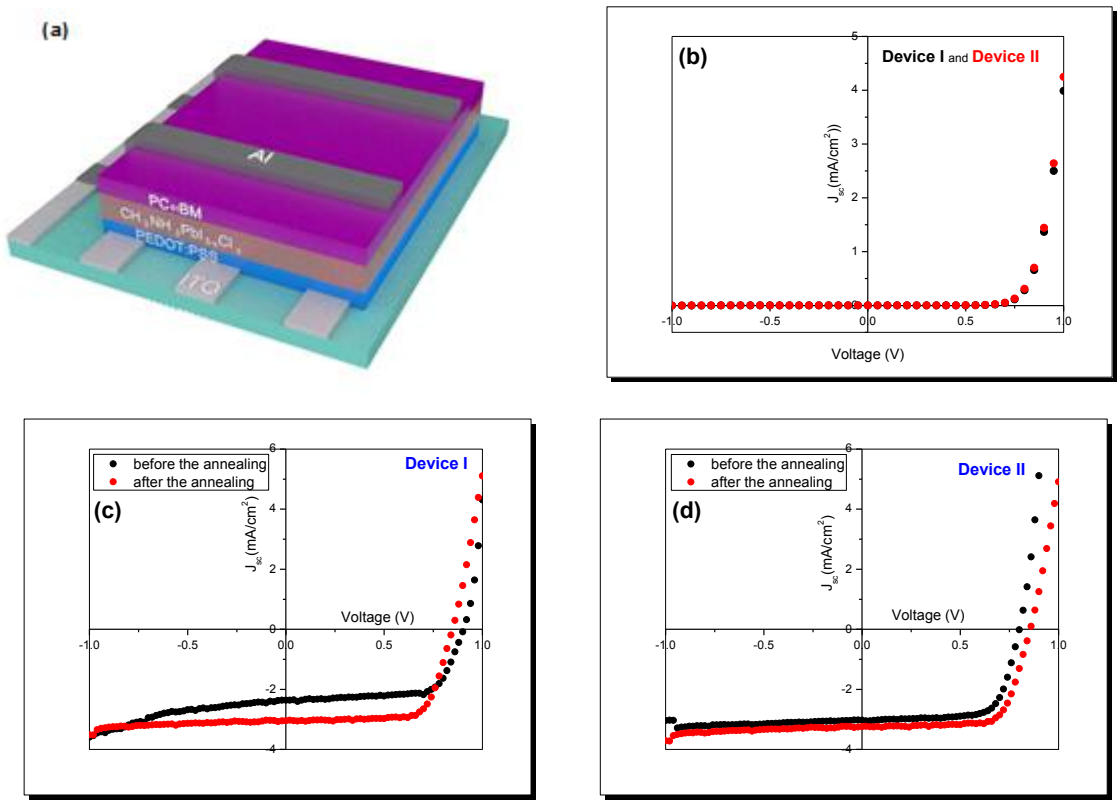

Fig.3. (a) Configuration of the solar cell in this study. (b) J – V curves of the cells in the dark after the annealing. (c) and (d) J – V curves of the cells under AM 1.5G simulated solar irradiation before and after the annealing.

4. Conclusion

In summary, we have developed the energy conversion efficiency of the organic-inorganic perovskite solar cells with the annealing after the fabrication. In spite of the photovoltaic efficiency was improved average 13%, which can be improved further optimization of the annealing processing. Therefore, we will systematically study effect of the annealing on the fabricated cells such as temperature and time.

References

[1] Jeng J Y, Chen K C, Chiang T Y, Lin P Y, Tsai T D, Chang Y C, Guo T F, Chen P, Wen T C and Hsu J 2014, Advanced materials, 26, 4107–4113.
[2] Jung H S and Park N G 2015, small, 11(1), 10–25.
[3] Kojima A, Teshima K, Shirai Y and Miyasaka T 2009, Journal of the American Chemical Society, 131 (17), 6050–6051.
[4] http://www.nrel.gov/ncpv/images/efficiency chart.jpg.
[5] Wu Z, Bai S, Xiang J, Yuan Z, Yang Y, Cui W, Gao X, Liu Z, Jin Y and Sun B 2014, Nanoscale 6, 10505–10510.
[6] Seo J, Park S, Kim Y C, Jeon N J, Noh J H, Yoon S C and Seok S 2014, Energy Environ. Sci., 7, 2642.
[7] Barrows A T, Pearson A J, Kwak C K, Dunbar A D F, Buckleya A R and Lidzey D G 2014, Energy Environ. Sci., 7, 2944.
[8] Chen Q, Zhou H, Hong Z, Luo S, Duan H S, Wang H-H, Liu Y, Li G and Yang Y 2014, J. Am. Chem. Soc. 136, 622−625.
[9] Chae J, Dong Q, Huang J and Centrone A 2015, Nano Lett., 15(12): 8114–8121.

[10] Liu M, Johnston M B and Snaith H J 2013, Nature 501,395–398.